In Vitro Platforms for the Study and Manipulation of Neutrophil Extracellular Traps
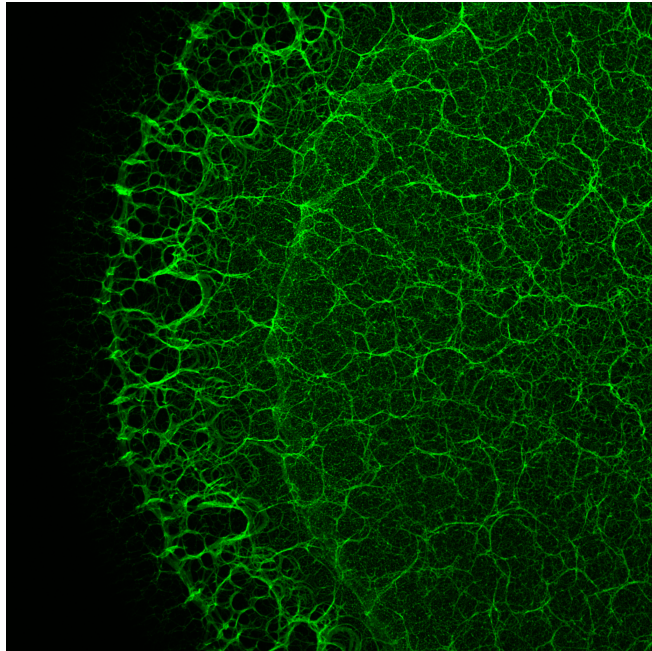
by

Cameron M. Louttit

A dissertation submitted in partial fulfillment
of the requirements for the degree of
Doctor of Philosophy
(Biomedical Engineering)
in the University of Michigan
2019

Doctoral Committee:

      Associate Professor James J. Moon, Chair
      Professor Omolola Eniola-Adefeso
      Assistant Professor Jason S. Knight
      Professor Lonnie D. Shea

Cameron M. Louttit

clouttit@umich.edu

ORCID iD: 0000-0002-8517-9278

Dedication

These pages detail scientific endeavors which were shared and supported at every step by the work of colleagues, contemporaries, and predecessors. What they fail to communicate, however, is the indescribable and indispensable support of the human behind those endeavors. This thesis is dedicated to all who carried me through this journey.

--

To my wife, who has stood by my side, kept me grounded, and loved me unconditionally through the heights of discovery and triumph and the throes of frustration and uncertainty.

To my family, old and new, who have enveloped me with love, remained steadfast in their constant support, and sacrificed untold amounts for my good.

To my extended family at St. Thomas, who have kept me anchored in the truth in every season.

To my friends near and far, who have shared in one way or another this journey with me.

To the glory of God, who provides in the most beautiful and mysterious of ways, and who makes all things work together for our ultimate and eternal good.

Acknowledgements

This work would not have been possible without the opening of the door to pursue it. I would therefore like to firstly thank Dr. James Moon for being willing to take me on as a student and for providing the time, space, and opportunity to explore exciting new ideas in one of the most fast-paced and enthralling pockets of our field. Additionally, Dr. Shuichi Takayama served as a co-advisor for the majority of the work presented here and provided substantial insight across the years. Thank you both for giving me the opportunity to research with you and grow as a scientist. Thank you also to my committee members, Dr. Lola Eniola-Adefeso, Dr. Jason Knight, and Dr. Lonnie Shea, for your helpful feedback and advice in the planning, execution, and interpretation of this work. Lastly, I would be remiss if I did not thank Dr. Richard Price and Dr. Kelsie Timbie at the University of Virginia for their formative mentorship in my early research career and their support of my graduate school pursuit.

Truly, science is a team sport – at least good science – and the work presented here is no exception. Thank you to all of the collaborators with whom I have worked, closely or distantly, recently or long ago, on the work presented here and the work that preceded and supported it. A profound thank you to the NET team – Priyan, Tai, Midori, Yang, Suny, Luke, and Paul – for your hard work and insights over these past few years. Our project has changed time and time again in that span, but it was built on (and continues to be carried by) each of you in one form or another. Thank you also to each member of the Moon Lab, past and present – Ali, Charlie, Cheng, Emeka, Joe, Jin, Jutaek, Kai, Lindsay, Luke, Łukasz, Marisa, Paul, Rui, Sejin, Xiaoqi, Yao, Yonghyun, and Yuchen – for your help, advice, and friendship. It was an honor to do

science alongside you all. I would like to especially highlight and thank Łukasz for patiently answering my innumerable questions, particularly in my early days; Sejin for both her advice and her scientific contributions to this work; and Charlie and Emeka for their profound friendship both in and out of lab.

I would like to also express my gratitude to the Department of Biomedical Engineering, a community which left a lasting impression on me from my first days on campus. To Maria Steele and the entire BME administrative staff, thank you for your tireless work to ensure smoothest waters for the students in this department. To my professors and GSIs, thank you for your immense contributions to this community of learning. To my cohort, the GSC, and all other friends, classmates, and colleagues, thank you for your conversations, scientific or otherwise, and your contributions to a culture of collegiality, collaboration, and fun.

Table of Contents

List of Figures

Abstract

Though only recently discovered, neutrophil extracellular traps (NETs) have rapidly attracted scientific and clinical interest as a potent weapon in the arsenal of innate immunity. These structures, fibers of decondensed nuclear material on which neutrophils localize their vast antimicrobial and proinflammatory stores, are released into sites of inflammation or injury with the presumed aim of constraining and clearing bacteria. It has also been shown, however, that NETs cause substantial harm, contributing to the pathogeneses of autoimmune diseases, cancers, and thrombotic disorders as well as inciting non-specific inflammation and collateral host damage. Thus, NETs as currently understood represent a paradox in which protection seems to be outweighed by detriment. In this light, fundamental questions have arisen surrounding the identity, function, and utility of NETs *in vivo*. This work describes two novel platforms rationally designed to assist in understanding and contextualizing this paradox.

In the first approach, aimed at better understanding NET identity and function, a reductionist *in vitro* assay framework was iteratively developed to study NETs from the bottom up, beginning first with their DNA-histone fibrous substructure. Precise control of DNA-histone complexation yielded a robust, reproducible, and scalable structure that stood in stark contrast to low-yield and heterogeneous NET preparations. These structures, termed DNA-histone mesostructures (DHMs), mirrored both NET morphology and, to an extent, function. In doing so, DHMs provided a novel assay platform which elucidated the significant role of the isolated NET backbone in common NET-associated phenomena, such as bacterial trapping and immune activation. In addition, it permitted the confirmation and quantification of the role of the peptide

LL-37 in altering NET degradation behavior. Beyond these structural studies, DHMs also yielded novel cell-based assays, including efforts to characterize the interaction between NET components and the immune system. Such studies elucidated the key role of DNA-histone synergism in NET-mediated immunostimulation, particularly amplified by the structural inclusion of non-methylated DNA. Additionally, they highlighted the importance of cell-structure proximity and contact in immune cell uptake and activation.

In the second approach, aimed at addressing the perceived pathophysiological imbalance mediated by NETs, a nanoparticulate platform was leveraged to modify cell-derived NETs *in vitro* with the aim of ultimately modifying them *in situ*. The chosen nanoparticles, hollow nanocapsules composed of polysaccharide, were internalized into neutrophils but avoided immediate NET induction; instead, they primed neutrophils for enhanced NET production only after classical stimulation. NETs produced by nanocapsule-loaded neutrophils displayed colocalization between particles and NET fibers, thereby indicating successful modification of NETs and promise for future therapeutic engineering of these structures.

Though distinct in motivation and design, these two platforms demonstrate novel approaches to understanding NETs and have revealed substantial insights about NET identity, function, and utility as described in this work. For both, the simultaneous youth and breadth of the NET field provide a profoundly large and diverse application base. Further studies leveraging both NET-mimicking *in vitro* assay platforms and NET-modifying nanoparticles will therefore continue to assist in the determination of both foundational and therapeutic NET biology.

Chapter 1: Introduction

1.1   A Brief Treatment of Classical Neutrophil Effector Biology

Neutrophils, also known as polymorphonuclear cells (PMNs), serve as a physiological first wave of defense against insult and injury. At the prompting of combinatorial damage- and pathogen-associated molecular patterns (DAMPs, PAMPs) indicative of cellular damage and pathogenic presence, respectively, as well as chemokines produced by locally-stationed immune cells, neutrophils are recruited in substantial numbers from the blood to the tissue[1]. There, these professional phagocytes both specifically and non-specifically engulf their surroundings and remain receptive to DAMPs or PAMPs in the environment, potentially triggering alternative effector functions. The breadth of this response, in addition to neutrophils' primacy of place as the first cells to be recruited from the blood, render them influential in initiating or quelling multiple subsequent immune processes.

In their capacity as professional phagocytes, neutrophils provide for both the elimination of extracellular pathogens as well as their degradation and presentation to adaptive immune cells for a finer-tuned response. Entities internalized into the neutrophilic phagosome are rapidly exposed to a variety of potent antimicrobial compounds, as intracellular granules fuse with the phagosomal compartment[2], as well as a variety of reactive oxygen species[3]. In addition, neutrophils have shown a modest ability to proteolytically degrade and present samples from the extracellular milieu to neighboring T and B cells. This process can occur either through a non-canonical vacuolar loading of major histocompatibility class I (MHC-I) or a "regurgitation" of peptide fragments for re-loading and presentation by neighboring antigen-presenting cells

(APCs)[4]. Outside of this classical phagocytosis role, neutrophils can also route their potent granular stores to the extracellular environment rather than the phagolysosome. While destructive to the host and therefore tightly regulated, this response is regarded as a time-delayed safety mechanism to destroy larger amounts of pathogens than any one neutrophil can internalize[1,5]. In parallel with both phagocytosis and degranulation, neutrophils coordinate subsequent responses by the production of pro-inflammatory cytokines and chemokines, recruiting and activating the next wave of immune subpopulations[6].

1.2   The Discovery and Characterization of Neutrophil Extracellular Traps

In 2004, a third arm was added to the canonical listing of neutrophilic effector functions: the production of neutrophil extracellular traps (NETs), filamentous meshworks of decondensed nuclear material decorated with the potent arsenal of neutrophilic protein and peptide components[7] (**Figure 1-1**). In a similar modality as degranulation, neutrophils leverage these structures to affect a broader level of damage than that attainable via phagocytosis. In producing NETs, neutrophils undergo one of several stepwise processes. While debate is ongoing regarding the mechanistic underpinnings of these processes, particularly as it relates to pathways unique to each subset of NET production, there are two broad subclasses: vital and non-vital NET production[8]. It should be noted here that among the ongoing debates in the field is the terminology that has developed in the 15 years since NETs were discovered. Despite the reliance in previous literature on the term "NETosis" to describe a distinct cell death pathway wherein NETs are expelled[9], a term that was even adopted by the Nomenclature Committee on Cell Death[10,11], a recent consortium of prominent NET authors discouraged its continued usage[12]. Thus, this work will omit this terminology in favor of "NET production", which encompasses both vital and non-vital NET-associated processes.

Non-vital or "suicidal" NET production was the first modality reported and the genesis of the term "NETosis". In this framework, neutrophils first decondense their nuclear material in a process catalyzed by the enzymes neutrophil elastase (NE), myeloperoxidase (MPO), and peptidyl arginine deiminase 4 (PAD4)[13,14]. The nuclear membrane is then broken down, giving way to a mixing of chromatin mesh and components from the granules and cytosol[15]. Finally, the NET is expelled into the extracellular space, with concomitant neutrophil death (**Figure 1-2**). Alongside reporting of this framework was a proposition of its function: as some of the primary initial stimuli identified were bacteria, including *Staphylococcus aureus, Shigella flexneri,* and *Staphylococcus typhimurium*, and these bacteria were found to be entrapped in NETs and displayed decreased colony-forming units (CFUs) after exposure, NETs were purported to be deployed to constrain and kill pathogens[7,16]. This theory was later bolstered by the finding that NET-mediated bacterial trapping was vital to preventing septic dissemination into the bloodstream[17,18].

In the following years, NET biology proved to be much more complex than initially proposed. The first reports of "vital" NET production appeared in 2009, describing NET structures which are released rapidly and independently of cell death[19]. It would later be shown that neutrophils producing these structures remain as functional "anuclear cytoplasts", entities which still migrate and phagocytose effectively but have lost their nuclear cargo to a non-lytic export of NETs[20]. While some progress has been made in demarcating the stimuli corresponding to each modality of NET production[8], much remains to be established in terms of mechanistic and functional understanding of these distinct structures. The current knowledge of these two discrete forms of NET formation is summarized in **Figure 1-3**.

It should also be noted that NET-like structures have been reported in a variety of cell types since their discovery in 2004. Other myeloid cells, such as eosinophils[21,22], basophils[22], and monocytes[23] can produce extracellular trap structures; in addition, lymphocytes were shown to produce NET-like structures, albeit in limited conditions with a synthetic oligonucleotide stimulus[24]. These findings have yielded a due increase in the scope of NET-related research and have encouraged the adoption of the broader umbrella term "extracellular trap" (ET)[12]; in this work, however, the "NET" designation will be kept since all experiments and comparisons were performed with neutrophils.

1.3 Neutrophil Extracellular Traps in Pathology

Despite the promise of NETs in constraining and potentially killing bacteria, and their apparent conservation both across cell types and phylogenetic classifications[25], these structures have proved paradoxical due to the immense harm that they can inflict to the host. As noted previously, the neutrophilic arsenal is regarded as a low-fidelity and high-power system, unleashing potent effector functions often without pristine specificity. In the case of NETs, however, the detrimental neutrophilic footprint is amplified by the persistence time of these structures. It is the combinatorial duty of deoxyribonucleases (DNases) and professional phagocytes to clear NETs after formation[26], a process that can be limited in diseases such as systemic lupus erythematosus (SLE) in which DNases are defective and NETs overabundant[27,28]. Even in disease states not associated with DNase impairment, however, NETs can cause profound harm. The complexation of polycations with DNA has been shown to render the resultant structures both resistant to enzymatic digestion[29] and, perhaps relatedly, potently immunogenic[30,31]. This phenomenon, and particularly the concomitant activation of immune subpopulations such as plasmacytoid dendritic cells (pDCs)[30,31], myeloid dendritic cells

(mDCs)[32,33], T lymphocytes (T cells)[34], and macrophages[35], has negatively implicated NETs in the perpetuation of a wide variety of immune disorders: examples include but are not limited to SLE[28,31], its related condition lupus nephritis[27], rheumatoid arthritis[32,36], autoimmune-associated small-vessel vasculitis[37], and Type 1 diabetes[38]. In many of these conditions, the inflammatory milieu around NETs promotes the generation of autoimmunity against these very structures, resulting in anti-neutrophil cytoplasmic antibodies (ANCAs)[33], anti-dsDNA antibodies[27], and antibodies directed against NET or extracellular matrix (ECM) components modified by NET-associated enzymes[36].

Interestingly, NET-associated harm is not only ascribed to immune disorders. These structures have been shown to capture circulating tumor cells from the vasculature, providing vessel wall anchors for the establishment of metastatic cancer in the liver sinusoids[39]. External to the vasculature, interstitial NETs prime pre-metastatic sites, encouraging the migration and proliferation of cancer cells[40] and enzymatically manipulating the ECM to awaken dormant tumor cells and ease their movement[41]. NET-associated enzymes and histones are potent and nonspecific inducers of damage, which often leaves collateral harm to host tissue after release[42,43]. Lastly, NETs serve as scaffolds which attract activated platelets and erythrocytes towards the formation of blood clots, potentially resulting in deep-vein thrombosis (DVT)[44,45].

1.4   Modern Critiques of Neutrophil Extracellular Traps

Thus, a paradoxical mosaic is assembled from the fragments of current NET knowledge. These structures, conserved and exhibited across a variety of hosts and cell types, appear to be vitally important for the spatiotemporal containment and clearance of bacteria; simultaneously, however, they also appear deleterious in a wide array of seemingly unrelated pathologies. That the current state of knowledge appears skewed towards the harmful is reflected in recent

critiques of NETs, with some authors questioning their sensibility as an evolutionarily inherited construct[46–48]. Bolstering these concerns is the demonstrated inability of the field to settle both on a particular mechanism of NET formation, as described above, as well as the baseline contents of NETs[49,50]. Synthesizing these various perspectives, it can be said that the modern debate surrounding NETs finds its root in three pillars: questions of NET identity, function, and utility to the host.

In an attempt to address each of these foundational concerns, it has been suggested that structures identified as NETs may in fact comprise several structurally and biochemically distinct nucleoprotein-based fibrous entities[46,51,52]. Such a theory is not lacking in historical precedent, as nucleoprotein-based complexes have, long before the discovery of NETs, been known to exist in serum both at physiological baseline and, to a heightened degree, in disease[53]. These complexes, often born out of the necrotic chaos at the epicenter of an inflammatory response, are inherently stochastic in their contents and roles. Their potential confusion with NETs could help to explain conflicting structural, compositional, and functional data and conclusions. As yet, however, formal definitions or dichotomies to this end have not reached a scientific consensus.

Fifteen years on, the NET field therefore sits at a crossroads. Vast clinical interest is counterbalanced by criticism, mostly aimed at the inability to establish both the foundational substance and function of a NET (or, more broadly, an ET). The aim of this thesis was to construct rationally designed platforms which could lend insight into NETs in each of the three categories of debate listed above: NET identity, function, and utility to the host. Through the first platform, described in Chapters 2 and 3, we iteratively developed a cell-free NET-mimicking structure focused on clarifying NET identity and function. This structure, and the *in vitro* assays that it enabled, revealed novel information about the DNA-histone backbone of NETs and its

critical role in NET morphology and behavior. Additionally, experiments utilizing this platform allowed the probing of individual NET-associated entities for structural and functional implications, an approach unattainable with cell-derived structures. In the second platform, reported in Chapter 4, we successfully altered cell-derived NETs from within using nanoparticles. Future studies leveraging this framework could encapsulate in NET-associated particles a variety of therapeutic entities, thereby improving the utility of NETs to the host in a range of pathophysiological settings.

1.5 Figures
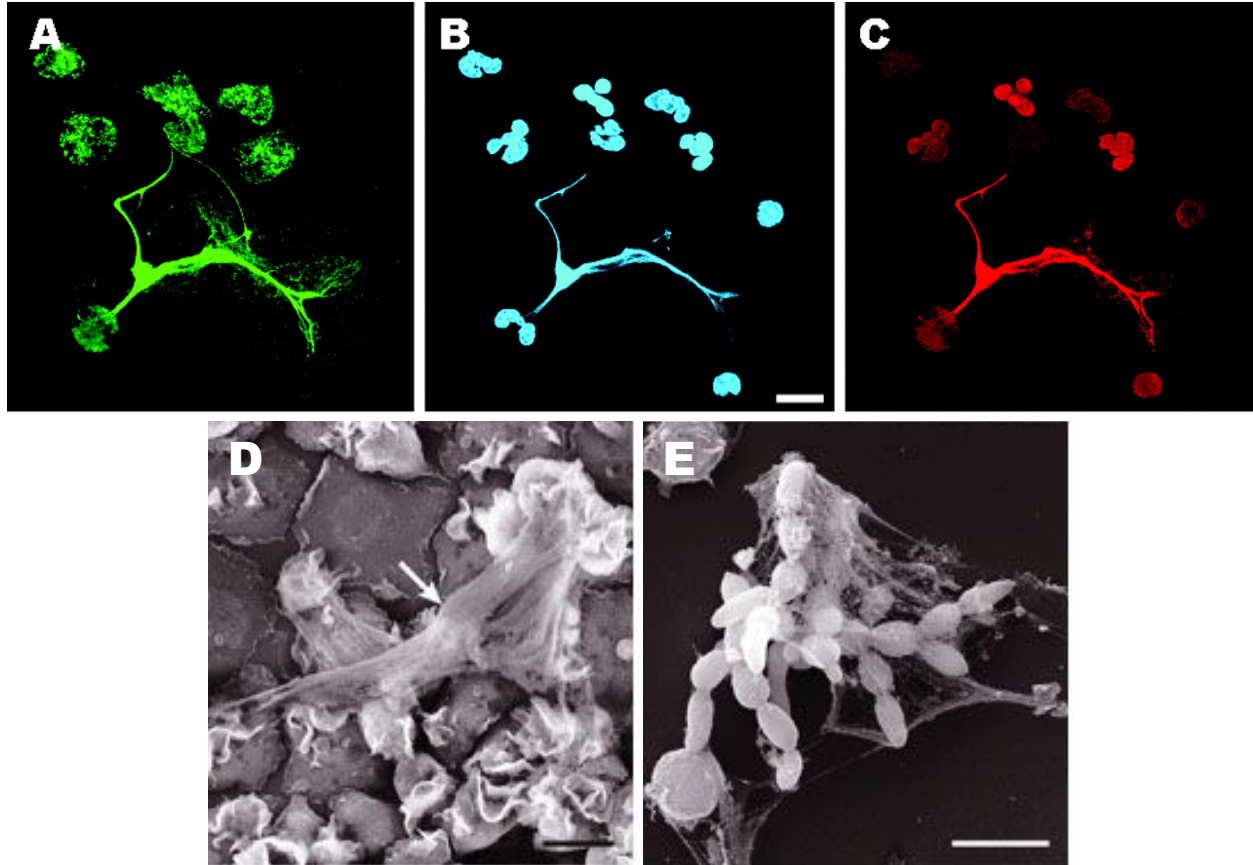
Figure 1-1: Depictions of NETs in the early literature

Assembled above are various visualizations of NETs in preliminary literature. (A-C) depicts immunostaining of NET fibers, wherein staining of neutrophil elastase (A), DNA (B), and the H2A-H2B-DNA complex (C) colocalize. (D-E) depicts NETs under scanning electron microscopy, both focusing on the producing neutrophil (D) and *C. albicans* entrapped in the NET fibers (E). Scale bars represent 10 μm in all images. (A-C) are reproduced in modified form from [7] and (D-E) are reproduced in modified form from [15].
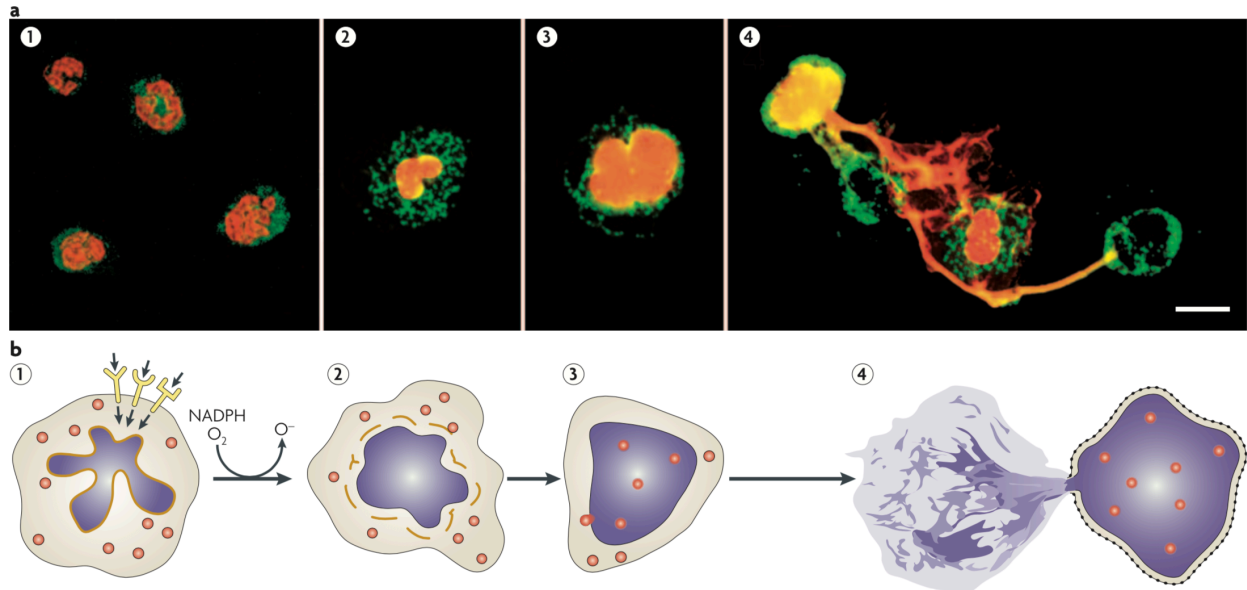
Figure 1-2: Formation process of classical "lytic" NET production

Aligned step-by-step formation processes for "lytic" NET production in (A) immunofluorescence (IF) images and (B) schematic form, reproduced from early NET literature. (1) Neutrophils at rest are activated by a given stimulus, catalyzing the production of reactive oxygen species by NADPH oxidase. (2) Nuclear membrane disintegrates as the nuclear contents (yellow/red in IF) decondense and expand. (3) Granular (green in IF) and cytosolic contents mix with the decondensed nuclear fibers. (4) NETs are ejected from the cell via plasma membrane rupture. Figure is reproduced in modified form from [15].
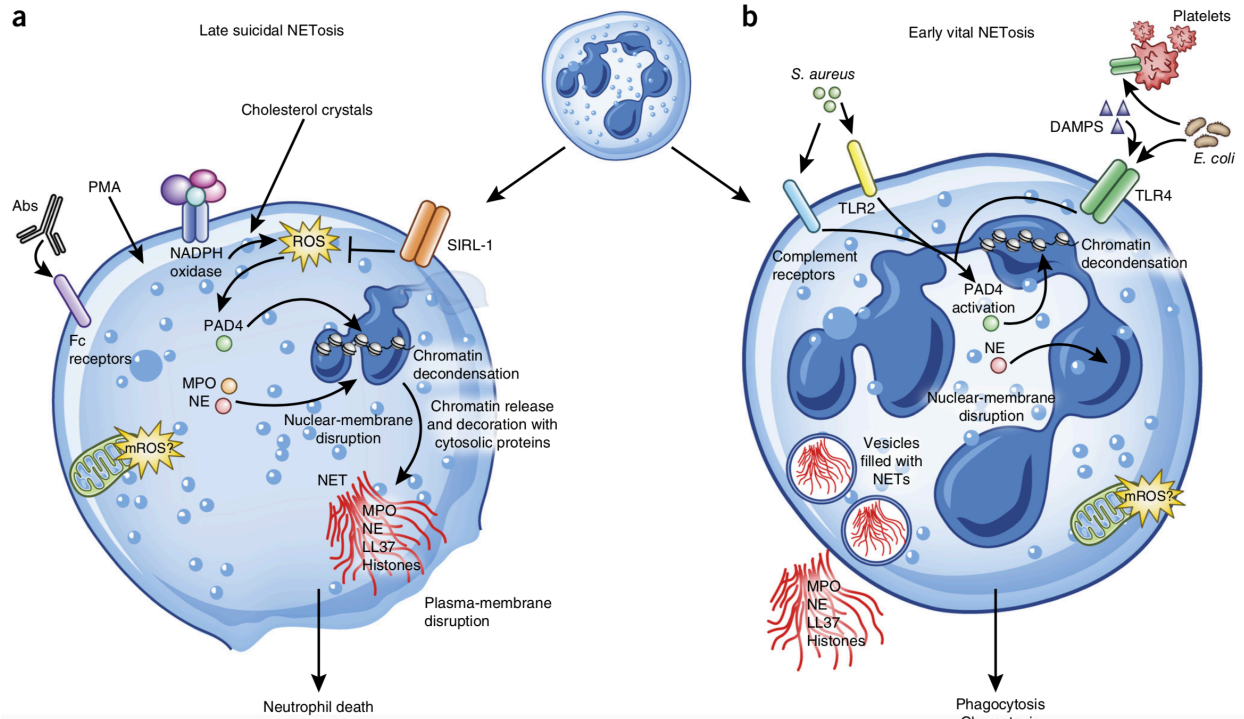
Figure 1-3: Dichotomy of lytic and vital NET production

A schematic indicating the current differentiations between lytic ("suicidal") and vital NET production, reproduced from recent NET literature. (A) Lytic NET production, in which decondensing nuclear contents expand into the cytoplasm and are released by rupture of the plasma membrane and consequent neutrophil death. (B) Vital NET production, in which NETs are exported into the extracellular space while maintaining cellular integrity, leaving an anuclear cytoplast still capable of migration and phagocytosis. Image reproduced from [8].

1.5   References

1.   Nathan, C. Neutrophils and immunity: challenges and opportunities. *Nat. Rev. Immunol.* **6**, 173–182 (2006).

2.   Hirsch, J. G. & Cohn, Z. A. Degranulation of polymorphonuclear leucocytes following phagocytosis of microorganisms. *J. Exp. Med.* **112**, 1005–1014 (1960).

3.   Hampton, M. B., Kettle, A. J. & Winterbourn, C. C. Inside the neutrophil phagosome: oxidants, myeloperoxidase, and bacterial killing. *Blood* **92**, 3007–3017 (1998).

4.   Potter, N. S. & Harding, C. V. Neutrophils Process Exogenous Bacteria Via an Alternate Class I MHC Processing Pathway for Presentation of Peptides to T Lymphocytes. *The Journal of Immunology* **167**, 2538–2546 (2001).

5.   Nathan, C. F. Neutrophil activation on biological surfaces. Massive secretion of hydrogen peroxide in response to products of macrophages and lymphocytes. *J. Clin. Invest.* **80**, 1550–1560 (1987).

6.   Scapini, P. *et al.* The neutrophil as a cellular source of chemokines. *Immunol. Rev.* **177**, 195–203 (2000).

7.   Brinkmann, V. Neutrophil Extracellular Traps Kill Bacteria. *Science* **303**, 1532–1535 (2004).

8.   Jorch, S. K. & Kubes, P. An emerging role for neutrophil extracellular traps in noninfectious disease. *Nature Medicine* **23**, 279–287 (2017).

9.   Fuchs, T. A. *et al.* Novel cell death program leads to neutrophil extracellular traps. *J. Cell Biol.* **176**, 231–241 (2007).

10.   Galluzzi, L. *et al.* Molecular definitions of cell death subroutines: recommendations of the Nomenclature Committee on Cell Death 2012. *Cell Death Differ.* **19**, 107–120 (2012).

11.   Galluzzi, L. *et al.* Molecular mechanisms of cell death: recommendations of the Nomenclature Committee on Cell Death 2018. *Cell Death Differ.* **25**, 486–541 (2018).

12.   Boeltz, S. *et al.* To NET or not to NET:current opinions and state of the science regarding the formation of neutrophil extracellular traps. *Cell Death Differ.* **26**, 395–408 (2019).

13.   Papayannopoulos, V., Metzler, K. D., Hakkim, A. & Zychlinsky, A. Neutrophil elastase and myeloperoxidase regulate the formation of neutrophil extracellular traps. *J. Cell Biol.* **191**, 677–691 (2010).

14.   Lewis, H. D. *et al.* Inhibition of PAD4 activity is sufficient to disrupt mouse and human NET formation. *Nat. Chem. Biol.* **11**, 189–191 (2015).

15.   Brinkmann, V. & Zychlinsky, A. Beneficial suicide: why neutrophils die to make NETs. *Nat. Rev. Microbiol.* **5**, 577–582 (2007).

16.   Urban, C. F., Reichard, U., Brinkmann, V. & Zychlinsky, A. Neutrophil extracellular traps capture and kill Candida albicans yeast and hyphal forms. *Cell. Microbiol.* **8**, 668–676 (2006).

17.   Clark, S. R. *et al.* Platelet TLR4 activates neutrophil extracellular traps to ensnare bacteria in septic blood. *Nat. Med.* **13**, 463–469 (2007).

18.   McDonald, B., Urrutia, R., Yipp, B. G., Jenne, C. N. & Kubes, P. Intravascular Neutrophil Extracellular Traps Capture Bacteria from the Bloodstream during Sepsis. *Cell Host & Microbe* **12**, 324–333 (2012).

19.   Yousefi, S., Mihalache, C., Kozlowski, E., Schmid, I. & Simon, H. U. Viable neutrophils release mitochondrial DNA to form neutrophil extracellular traps. *Cell Death & Differentiation* **16**, 1438–1444 (2009).

20.   Yipp, B. G. *et al.* Infection-induced NETosis is a dynamic process involving neutrophil multitasking in vivo. *Nat. Med.* **18**, 1386–1393 (2012).

21.   Yousefi, S. *et al.* Catapult-like release of mitochondrial DNA by eosinophils contributes to antibacterial defense. *Nature Medicine* **14**, 949–953 (2008).

22.   Schorn, C. *et al.* Monosodium urate crystals induce extracellular DNA traps in neutrophils, eosinophils, and basophils but not in mononuclear cells. *Front. Immunol.* **3**, (2012).

23.   Granger, V. *et al.* Human blood monocytes are able to form extracellular traps. *J. Leukoc. Biol.* **102**, 775–781 (2017).

24.   Ingelsson, B. *et al.* Lymphocytes eject interferogenic mitochondrial DNA webs in response to CpG and non-CpG oligodeoxynucleotides of class C. *Proc. Natl. Acad. Sci. U.S.A.* **115**, E478–E487 (2018).

25.   Zhang, X., Zhuchenko, O., Kuspa, A. & Soldati, T. Social amoebae trap and kill bacteria by casting DNA nets. *Nature Communications* **7**, 10938 (2016).

26.   Farrera, C. & Fadeel, B. Macrophage clearance of neutrophil extracellular traps is a silent process. *J. Immunol.* **191**, 2647–2656 (2013).

27.   Hakkim, A. *et al.* Impairment of neutrophil extracellular trap degradation is associated with lupus nephritis. *Proc. Natl. Acad. Sci. U.S.A.* **107**, 9813–9818 (2010).

28.   Leffler, J. *et al.* Neutrophil extracellular traps that are not degraded in systemic lupus erythematosus activate complement exacerbating the disease. *J. Immunol.* **188**, 3522–3531 (2012).

29.   Neumann, A. *et al.* Novel role of the antimicrobial peptide LL-37 in the protection of neutrophil extracellular traps against degradation by bacterial nucleases. *J Innate Immun* **6**, 860–868 (2014).

30.   Lande, R. *et al.* Plasmacytoid dendritic cells sense self-DNA coupled with antimicrobial peptide. *Nature* **449**, 564–569 (2007).

31.   Lande, R. *et al.* Neutrophils Activate Plasmacytoid Dendritic Cells by Releasing Self-DNA–Peptide Complexes in Systemic Lupus Erythematosus. *Science Translational Medicine* **3**, 73ra19-73ra19 (2011).

32.   Papadaki, G. *et al.* Neutrophil extracellular traps exacerbate Th1-mediated autoimmune responses in rheumatoid arthritis by promoting DC maturation. *Eur. J. Immunol.* **46**, 2542–2554 (2016).

33.   Sangaletti, S. *et al.* Neutrophil extracellular traps mediate transfer of cytoplasmic neutrophil antigens to myeloid dendritic cells toward ANCA induction and associated autoimmunity. *Blood* **120**, 3007–3018 (2012).

34.   Tillack, K., Breiden, P., Martin, R. & Sospedra, M. T Lymphocyte Priming by Neutrophil Extracellular Traps Links Innate and Adaptive Immune Responses. *The Journal of Immunology* **188**, 3150–3159 (2012).

35.   Warnatsch, A., Ioannou, M., Wang, Q. & Papayannopoulos, V. Neutrophil extracellular traps license macrophages for cytokine production in atherosclerosis. *Science* **349**, 316–320 (2015).

36.   Khandpur, R. *et al.* NETs Are a Source of Citrullinated Autoantigens and Stimulate Inflammatory Responses in Rheumatoid Arthritis. *Science Translational Medicine* **5**, 178ra40-178ra40 (2013).

37.   Kessenbrock, K. *et al.* Netting neutrophils in autoimmune small-vessel vasculitis. *Nature Medicine* **15**, 623–625 (2009).

38.   Wong, S. L. *et al.* Diabetes primes neutrophils to undergo NETosis, which impairs wound healing. *Nature Medicine* **21**, 815–819 (2015).

39.   Cools-Lartigue, J. *et al.* Neutrophil extracellular traps sequester circulating tumor cells and promote metastasis. *Journal of Clinical Investigation* **123**, 3446–3458 (2013).

40.   Park, J. *et al.* Cancer cells induce metastasis-supporting neutrophil extracellular DNA traps. *Science Translational Medicine* **8**, 361ra138-361ra138 (2016).

41.   Albrengues, J. *et al.* Neutrophil extracellular traps produced during inflammation awaken dormant cancer cells in mice. *Science* **361**, (2018).

42.   Saffarzadeh, M. *et al.* Neutrophil extracellular traps directly induce epithelial and endothelial cell death: a predominant role of histones. *PLoS ONE* **7**, e32366 (2012).

43.   Villanueva, E. *et al.* Netting Neutrophils Induce Endothelial Damage, Infiltrate Tissues, and Expose Immunostimulatory Molecules in Systemic Lupus Erythematosus. *The Journal of Immunology* **187**, 538–552 (2011).

44.   Fuchs, T. A. *et al.* Extracellular DNA traps promote thrombosis. *Proceedings of the National Academy of Sciences* **107**, 15880–15885 (2010).

45.   Wolach, O. *et al.* Increased neutrophil extracellular trap formation promotes thrombosis in myeloproliferative neoplasms. *Sci Transl Med* **10**, (2018).

46.   Nauseef, W. M. & Kubes, P. Pondering neutrophil extracellular traps with healthy skepticism. *Cellular Microbiology* **18**, 1349–1357 (2016).

47.   Malachowa, N., Kobayashi, S. D., Quinn, M. T. & DeLeo, F. R. NET Confusion. *Frontiers in Immunology* **7**, (2016).

48.   Yousefi, S. & Simon, H.-U. NETosis – Does It Really Represent Nature's "Suicide Bomber"? *Frontiers in Immunology* **7**, (2016).

49.   Urban, C. F. *et al.* Neutrophil extracellular traps contain calprotectin, a cytosolic protein complex involved in host defense against Candida albicans. *PLoS Pathog.* **5**, e1000639 (2009).

50.   Lim, C. H. *et al.* Thrombin and Plasmin Alter the Proteome of Neutrophil Extracellular Traps. *Front Immunol* **9**, 1554 (2018).

51.   Konig, M. F. & Andrade, F. A Critical Reappraisal of Neutrophil Extracellular Traps and NETosis Mimics Based on Differential Requirements for Protein Citrullination. *Front Immunol* **7**, 461 (2016).

52.   Desai, J., Mulay, S. R., Nakazawa, D. & Anders, H.-J. Matters of life and death. How neutrophils die or survive along NET release and is 'NETosis' = necroptosis? *Cell. Mol. Life Sci.* **73**, 2211–2219 (2016).

53.   Holdenrieder, S. *et al.* Circulating nucleosomes in serum. *Ann. N. Y. Acad. Sci.* **945**, 93–102 (2001).

Chapter 2: NET-Mimicking Structure Formation at the Interface of an Aqueous Two-Phase System

2.1 Introduction

The first chapter of this work expounded upon the immense immunobiological and clinical interest surrounding NETs but also indicated the contemporary concerns aimed at the core of the NET field. Despite the importance of these questions, they have remained challenging to study due to the heterogeneity, complexity, and fragility of NETs. As previously discussed, NETs contain a diverse assortment of proteins and peptides, a catalogue which seems to vary based on neutrophil source, stimulus, and disease state[1–3]. This variance both encourages the aforementioned questions about NET identity and also hinders reproducibility across studies. Even if NETs were ascribed a standard grouping of proteins and peptides, however, the sheer complexity of these structures renders mechanistic studies challenging. Many components of NETs exhibit multiple functions pathophysiologically; some even eschew their canonical roles in the context of the NET framework[4]. For several key components, removal or inhibition completely abolishes the ability of neutrophils to produce NETs, rendering their isolated study impossible with current methods[5,6]. In total, NETs as currently studied appear as more or less a "black box". The implications of their presence and absence can be deduced via systemic administration of DNase or inhibitors of PAD4 and/or neutrophil elastase (NE), but the mechanistic responsibilities of any one component in the NET framework cannot be elucidated.

Lastly, these challenges are compounded by the logistical difficulty of obtaining NETs to study. In an article describing the optimal isolation procedures, the group that first reported

NETs in 2004 stated that "NETs are very fragile even after fixation and have to be manipulated with great care, otherwise the majority will get lost during the preparation"[7]. In another similar article, authors warned of the challenges associated with primary neutrophils, stating that these cells "may be accidentally activated during the process of isolation leading to apoptosis", a common end result that drastically decreases the NET yield[8]. Thus, it was evident that an alternative framework to study NETs was necessary. Ideally, such a platform would avoid the use of primary neutrophils and would counterbalance the complexity and heterogeneity of cell-derived NETs with simplicity and reproducibility.

This chapter discusses the first of two iterative steps in the development of such a platform. In this first version, normally stochastic DNA and histone complexation was controlled across the interface of an aqueous two-phase system, yielding a reproducible structure which mirrored both NET morphology and, to an extent, behavior. Through this recapitulation, our structures are positioned as a novel *in vitro* assay platform with which to better understand the role of NET structural fibers and the individual components which decorate them *in vivo*.

2.2   Results and Discussion

2.2.1   *Preface*

As with all good science, the work of this thesis has been the result of extraordinarily collaborative efforts. In particular, the systems developed in this chapter and the next were achieved by a team spanning multiplate laboratories and, eventually, universities. The end product would not have been attained without each member of the team contributing unique insights, expertise, and efforts. These contributions are catalogued as thoroughly as possible in the "Attributions" section at the end of each chapter; however, it seemed only proper to raise this acknowledgement prior to the presentation of data as well.

2.2.2 DNA-Histone Admixing Forms a Controllable Fibrous Aggregate

While several studies on the protein and peptide composition of NETs have been undertaken[1,2] and have produced conflicting results, as described previously, nuclear material is a constant amongst all NETs and similar structures. It is noteworthy that these nuclear components are also predominant: one analysis reported histones to compose almost 70% of the total molar fraction of non-DNA NET components identified by mass spectrometry[1]. Indeed, in the classical framework of non-vital NET production, nuclear decondensation occurs first, followed by mixing of the structural mesh with various granular and cytosolic proteins which associate via unspecified (perhaps often electrostatic) mechanisms[9]. We therefore sought to mimic this earliest stage of NET formation, where decondensed DNA and histones form meshes on which the rest of the NET later assembles.

Prior experiments identified that DNA and histones, when combined in simple salt-containing solutions, form robust fibrous complexes which appear stochastic in nature (data not shown). This phenomenon has been previously studied at length, with particular treatment in modeling[10,11]. In order to first assess the characteristics of this complexation, DNA (derived from salmon sperm) and histones (calf thymus) were mixed in varying mass ratios in a 100 μL volume. Pre-labeling the DNA with 4',6-diamidino-2-phenylindole (DAPI) rendered the resulting structures visible via fluorescence microscopy. Imaging revealed DNA as the limiting factor by mass in formation of stable structures, with histones in excess (**Figure 2-1**). In addition, these experiments also identified 1 mg/mL as the minimum DNA concentration from which stable fibers could be derived in this configuration.

2.2.3 *Stable and Constrained DNA-Histone Structures are Formed via Controlled Diffusion*

In order to develop a stable and reproducible platform utilizing these DNA-histone fibers, it was necessary to control their creation and deposition. Towards this purpose, we employed an aqueous two-phase system (ATPS), a construct in which two aqueous solutions of specific polymers and/or salts are engineered to partition[12]. The ATPS paradigm is noteworthy for its ability to provide component separation without the use of harsh or denaturing solvents. Previous research has therefore described that ATPS frameworks are useful for compartmental isolation in biological systems[13] and that, in particular, the interface of the two phases can be employed to interact entities dissolved alongside one of the two separating polymers/salts[14]. We therefore sought to interact DNA and histones across the ATPS interface, employing the common formulation of poly(ethylene glycol) (PEG) and dextran (DEX) as our two separating polymers.

It is common among ATPS systems to determine much of the protocol empirically, as the number of factors which affect phase equilibration and separation are complex and ill-defined[12]. Thus, for a given two-polymer system, it is typical to explore various concentrations of each phase-separating component to determine which combinations will be necessary for robust phase separation. In this application, it was also necessary to include the two biological components, DNA and histones, to identify not only ATPS combinations which separated but which also facilitated the formation of robust DNA-histone structures. The initial constraints within which iterative and empirical development of this protocol occurred were (a) formation on the surface of a multi-well plate, and (b) the dehydration of one component-polymer combination in a circular footprint on the well surface before the addition of the second component-polymer combination. This second constraint was adopted to assist in the uniform deposition of material

in the well and to increase the interaction window, with interaction occurring both during

rehydration and equilibration/separation of the phases.

Initially, two component specifications for each ATPS-forming polymer were chosen for

comparison: solutions of 15% w/v 10 kDa and 10% w/v 500 kDa DEX, and solutions of 10%

w/v 8 kDa and 5% w/v 35 kDa PEG. These solutions were selected based on previous research

and screening (data not shown), and a preliminary qualitative experiment was undertaken to

examine structure formation utilizing each of these components. Because DEX has been

previously noted as a stabilizer for nucleic acid structures[15], DNA (lambda phage, methylated)

was combined with DEX such that its final concentration was 150 ng/μL. This solution was

spotted on a microwell plate and dehydrated for 24 hours, after which it was reconstituted in a

100 μL volume of 1 mg/mL calf thymus histones in the PEG solutions previously listed. Also

included in this solution was Sytox Green such that the resulting structure, which formed over

the course of 3 hours, could be visualized by fluorescence microscopy.

Each ATPS component combination resulted in fiber formation within a roughly circular

footprint; however, it was evident that the combination of 35 kDa PEG and 10 kDa DEX did not

produce a stable structure (**Figure 2-2**). As shown via the buffer control, the addition of DEX

was not necessary for the formation of a circular fibrous structure. DEX did, however, provide

for the formation of stronger bundles of fibers, a phenomenon which correlated with increased

DEX molecular weight. From these options, the combination of 35 kDa PEG and 500 kDa DEX

were chosen due to their formation of fibers which exhibited the most robust morphology at low

magnification (**Figure 2-2 A**) and regularity at high magnification (**Figure 2-2 B**).

A similar course of iterative qualitative experimentation was undertaken to explore

alternate routes of formation and component compositions. For example, in one such experiment,

the assignment of biological components (DNA, histones) to phase-separating polymers (PEG, DEX) was reversed to confirm the decision to combine DNA and DEX. When histone-DEX droplets were spotted and rehydrated with DNA-PEG solution, much weaker fibrous structures formed (**Figure 2-3**). Related experiments exploring parameters such as the concentration of biological components, volume of the spotted droplet, dehydration parameters, and brand and type of microwell plate were also executed in the pursuit of protocol optimization (data not shown).

In total, the optimized formulation was as follows: a solution of 100 ng/µL lambda phage DNA in 10% 500 kDa DEX was spotted at 5 µL in a 96-well plate and dehydrated for 24 hours, followed by the addition of 100 µL 1 mg/mL calf thymus histone in 5% 35 kDa PEG for 3 hours. After multiple changes of 50 µL 10 mM Tris-HCl to wash the well of residual and inert components, the DNA-histone structures were rendered ready for use (**Figure 2-4**). Structures generated by this protocol were found to be both wash-stable and reproducible (**Figure 2-5**).

Thus, it was found that the interaction of DNA and histones via controlled diffusion across the interface of a rehydrating ATPS allowed for the formation of stable DNA-histone structures. This protocol enabled precise control over an interaction process which was previously stochastic in nature and produced structures adhered to the surface of multiwell plates.

2.2.4   *ATPS-Formed DNA-Histone Structures Mimic NET Morphology*

After the establishment of a reproducible DNA-histone structure formation protocol, we sought to further understand the morphology of these structures and, in particular, their relation to NETs. Despite the reductionist nature of this platform and the lack of non-nuclear NET components, previous research indicated that DNA-histone fibers may have a morphological

similarity to NETs. Early NET authors described the ultrastructure, visible under scanning electron microscopy (SEM), as "beads on a string"[16] and noted its similarity to traditional extended chromatin observed under the same methodologies. Thus, it was possible that the creation of stable and reproducible structures of DNA-histone fibers could recapitulate the nanoscale morphology of NETs.

To investigate this possibility further, ATPS-formed DNA-histone structures were first visualized under high-resolution confocal microscopy after staining with Sytox Green. Despite the reproducible nature of the fibrous bundles visualized in the iterative development of these structures, morphology similar to NETs would consist of fibers much smaller in diameter; thus, a higher-powered microscopic analysis was necessary to parse the large bundles apart and, if possible, view fibers which were smaller and lighter-staining. This analysis revealed a "nanofibrous" morphology which served as the foundational structure of the DNA-histone meshwork; fibers of this size were not visible via traditional fluorescence microscopy (**Figure 2-6**). The presence of these fibers and their intricate patterns provided an indication that at the core of these DNA-histone structures were fibers possibly similar to those of cell-based NETs.

SEM was then employed to provide a finer view of the fiber size and shape. DNA-histone structures analyzed in this manner displayed the characteristic "beads on a string" morphology of traditional NETs (**Figure 2-7**). In addition, analysis of these images provided a range of diameters for both "beads" and "strings": approximately 10-20 nm for the "strings", and 70-90 nm for the "beads". These values correspond to those attributed to NETs in the literature[17], indicating qualitative and quantitative morphological consistency at the nanoscale between NETs and DNA-histone structures.

2.2.5 *DNA-Histone Structures Recapitulate NET Degradation Behaviors*

Having established that the morphology of ATPS-formed DNA-histone structures mirrored that of neutrophil-derived NETs, we sought to explore functional applications of such a structure. In particular, given the configuration of this platform in multiwell plates, we examined potential *in vitro* assays which could be built using these reproducible entities at their core. One such application was to determine the degradation behavior of the DNA-histone structure and explore entities which modified the kinetics associated with this process. Degradation of NET structures has been of particular recent interest since the discovery that lupus patients suffer from an inability to degrade NETs, both from defective serum nucleases and from autoantibodies that protect NETs from degradation[18,19]. In addition, it was found that strongly cationic components of the NET such as the peptide LL-37 serve to condense the structures and prevent their facile digestion by endogenous nucleases[4]. Together, these findings identified NET degradation and, in particular, entities which inhibited or slowed that process, as key factors in the pathogenic role of NETs. We therefore sought to leverage the multiwell-based DNA-histone structures towards the establishment of an *in vitro* assay examining this effect.

Firstly, it was necessary to establish that DNA-histone structure degradation could be reliably monitored. The multiwell plate attachment of these structures suggested that a microplate reader would be ideally suited for such a purpose; thus, structures were labeled with Sytox Green and comparatively monitored via microplate reader and imaged under fluorescence microscopy during digestion by soluble DNase I. Rapid degradation of the structures on the order of one hour was observed via imaging, wherein both the size and fluorescence intensity of the structure diminished (**Figure 2-8 A**; images contrast-enhanced to render structure visible at each time point). The corresponding microplate reader values for this degradation process

matched the behavior observed under imaging (**Figure 2-8 B**). Thus, the *in vitro* assay leveraging ATPS-formed DNA-histone structures to monitor degradation behaviors was validated.

Next, we sought to modify the degradation behavior of the DNA-histone structures and assess the extent to which this perturbation could be monitored and quantified. Building on the previous establishment of the NET-associated peptide LL-37 as an inhibitor of NET degradation[4], we incubated DNA-histone structures with 0, 0.5, 5, and 50 μM LL-37 for one hour post-formation. Structures were then washed, labeled with Sytox Green, and incubated with DNase I at 37°C with continuous monitoring via microplate reader. The kinetic degradation curves displayed a clear dose-dependent impairment of degradation by LL-37-containing structures (**Figure 2-9 A**). This inhibition was quantified through the identification of the degradation half-life, the time point at which structural fluorescence intensity reached one half of its initial value. Incubation of DHMs with 50 μM LL-37 increased half-life by a factor of 5.22 over control ($p < 0.0001$), while 5 μM LL-37 yielded a 1.9-fold increase ($p < 0.0001$) (**Figure 2-9 B**). While this data confirmed previous knowledge, that LL-37 slows DNase-mediated degradation of NETs, it also provided several novel advantages over previous studies. Firstly, such an assay was the first to observe the singular effect of LL-37 in a NET-mimicking framework. In addition, the reproducible and scalable nature of this platform enabled the generation of a higher-throughput assay than allowed by cell-derived NETs given their difficult isolation procedures and heterogeneity. This scalability rendered specific quantitative and statistically analyzable metrics to be generated examining the established phenomenon of NET degradation resistance.

2.3   Conclusions

Through the employment of a dehydration-rehydration ATPS framework, we were able to control the previously stochastic process of nucleic acid-histone complexation towards the production of stable, robust, fibrous structures. These structures mirror the morphology of NETs at the nanoscale and also recapitulate known NET functions such as degradation resistance upon complexation with cationic peptides. While we make no claim that this platform is identical to a NET given its minimalist composition, we also highlight that the reductionist nature of the DNA-histone structure permits a homogeneity and reproducibility previously impossible with neutrophil-derived NETs. Thus, these structures can be employed in multiwell plate-based assays to better understand the underlying structure and identity of NETs as well as the functional roles that various known NET-associated entities can assume in the context of that architecture.

2.4   Materials and Methods

DNA-histone admixture

DAPI-labeled DNA (salmon sperm, Sigma-Aldrich) and histones (calf thymus, Sigma-Aldrich) were prepared at 1 mg/mL in ultrapure water. In a 96-well plate, 50 μL DNA was added to multiple wells followed by 50 μL histones in a series of twofold dilutions in Tris ranging from 0-fold (1:1 histone:DNA) to 16-fold (1:16 histone:DNA). The inverse experiment was performed with serial dilutions of DNA being added to wells followed by 50 μL 1 mg/mL histones. The resultant fibers that formed were imaged under fluorescent microscopy (Nikon TiU microscope), and images were prepared in ImageJ (National Institutes of Health).

Iterative Development of ATPS Protocol

For preliminary experiments, dextran (10 kDa and 500 kDa MW, Sigma-Aldrich) and

PEG (8 kDa and 35 kDa MW, Sigma-Aldrich) were prepared at 2x concentrations (30% and

20% for DEX, respectively; 20% and 10% for PEG, respectively) in ultrapure water. These

solutions were mixed with DNA and histones prepared at 2x concentrations in ultrapure water

(300 ng/mL DNA, 2 mg/mL histones) in 1:1 volumetric ratios. In some experiments, DNA was

prelabeled with 5 µM Sytox Green prior to spotting; in others, Sytox Green was added to the

histone rehydration solution at the same concentration. 5 µL droplets of DNA/DEX (or

histone/DEX for the inverted assignment experiment) were deposited at the bottom of a

multiwell plate and dehydrated for 24 hours under vacuum. Droplets were then rehydrated with

100 µL histones/PEG (or DNA/PEG) for 2-3 hours, followed by serial washing steps with 10

mM Tris-HCl. The optimized protocol followed a similar formation procedure but utilized 100

ng/mL DNA in 10% (final) 500 kDa DEX and 1 mg/mL histones in 5% (final) 35 kDa PEG.

High-Resolution Imaging of DNA-Histone Structures

For confocal imaging, DNA-histone structures were prepared on plastic or glass

coverslips according to the optimized formulation described above. These structures were post-

stained with 5 µM Sytox Green, washed, and visualized with a Nikon A1Rsi laser scanning

confocal microscope.

For SEM, DNA-histone structures were prepared as previously described and fixed in 4%

paraformaldehyde (Electron Microscopy Services). After washing, structures were secondarily

fixed in 1% osmium tetroxide (Sigma-Aldrich), washed again, and dehydrated using a stepwise

sequence of ethanol solutions of 25%, 50%, 75%, 95%, and 100% at 10-15 minutes per solution.

Lastly, samples were dried via washing with and evaporation of hexamethyldisilazane (Electron Microscopy Services), sputter coated with gold, and imaged with a SEM/FIB (FEI Company).

Monitoring of DNA-Histone Structure Degradation

DNA-histone structures were prepared as previously described and post-stained with 5 µM Sytox Green. For LL-37 containing wells, LL-37 was prepared at the indicated concentrations and incubated with structures after washing for at least 1 hour; residual peptide was subsequently washed away. Wells were then aspirated of all liquid contents, which were replaced with 1 mg/mL DNase I (Sigma-Aldrich) in 10 mM Tris-HCl supplemented with calcium and magnesium. The plate was then placed in a microplate reader (Synergy NEO, Biotek) pre-warmed to 37°C and incubated for 30-90 mins with reads every 1-10 mins. Kinetic fluorescent intensities were normalized to the first signal measured for each structure, and the degradation half-life was calculated as the time at which normalized fluorescence intensity reached a value of $I = 0.5$.

Statistical Analysis

Statistics were acquired with GraphPad Prism 6.0 (GraphPad) using ANOVA tests with Tukey's multiple comparisons correction. Values are reported as mean ± SD unless otherwise indicated. Indicators of significance are as follows: * = $p < 0.05$, ** = $p < 0.01$, *** = $p < 0.001$, **** = $p < 0.0001$.

2.5 Acknowledgements and Attributions

As described in the Preface, the work presented herein was produced by a profoundly collaborative effort. The ATPS-based structures were an iterative development on a variety of precursor DNA-histone structures; the work of conceptualizing, testing, and validating these structures was an equal effort between C.L., Dr. Priyan Weerappuli (P.W.), and Dr. Taisuke Kojima (T.K.). ATPS was a particular expertise of T.K., who provided critical insight into the development of this platform; Cameron Yamanishi was also an invaluable resource to this end. Early formation and imaging work was split among C.L., P.W., and T.K., and the various experiments iteratively exploring protocol and parameter adjustments were distributed evenly. C.L. was most directly responsible for confocal imaging and post-processing, and P.W. was most directly responsible for SEM preparation and imaging. Generation of the microplate reader data and modification with LL-37 was an even contribution among all team members. There were also many experiments performed by each member which did not become figures presented or published but which inevitably aided in the development of this platform.
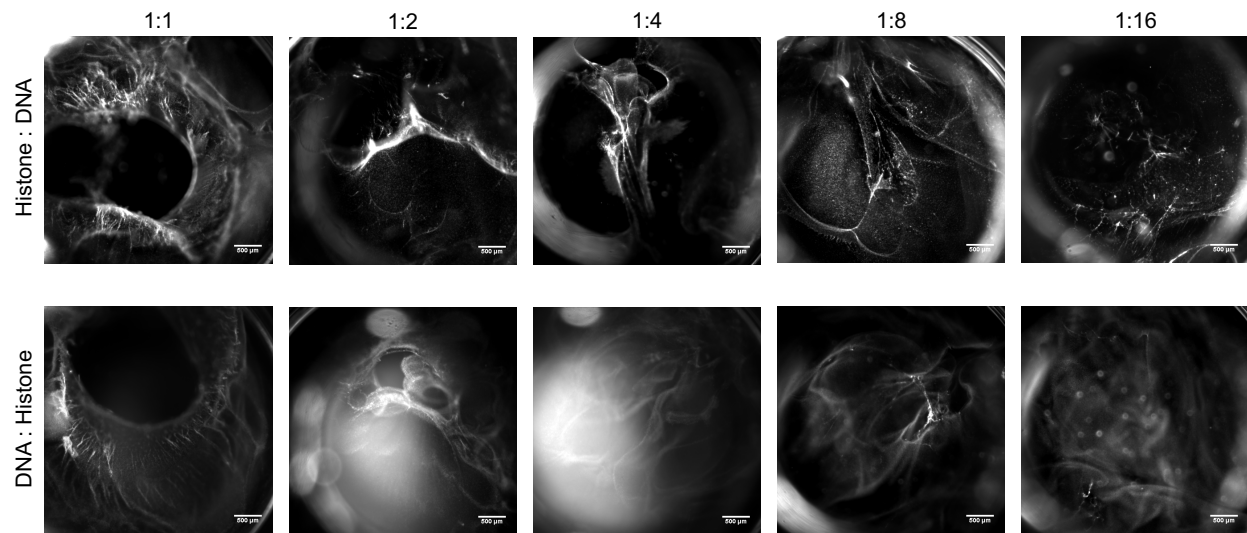
2.6   Figures

Figure 2-1 : DNA-histone fiber formation is controllable via titration

DAPI-labeled salmon sperm DNA and calf thymus histones were combined at the indicated concentration (mass) ratios, where constant component (right side of ratio) was maintained at 1 mg/mL and the changing component (left side) was serially diluted. The resultant structures, formed in 100 µL of 10 mM Tris-HCl buffer in a 96-well plate, were imaged with single-channel fluorescence microscopy. Scale bar represents 500 µm.
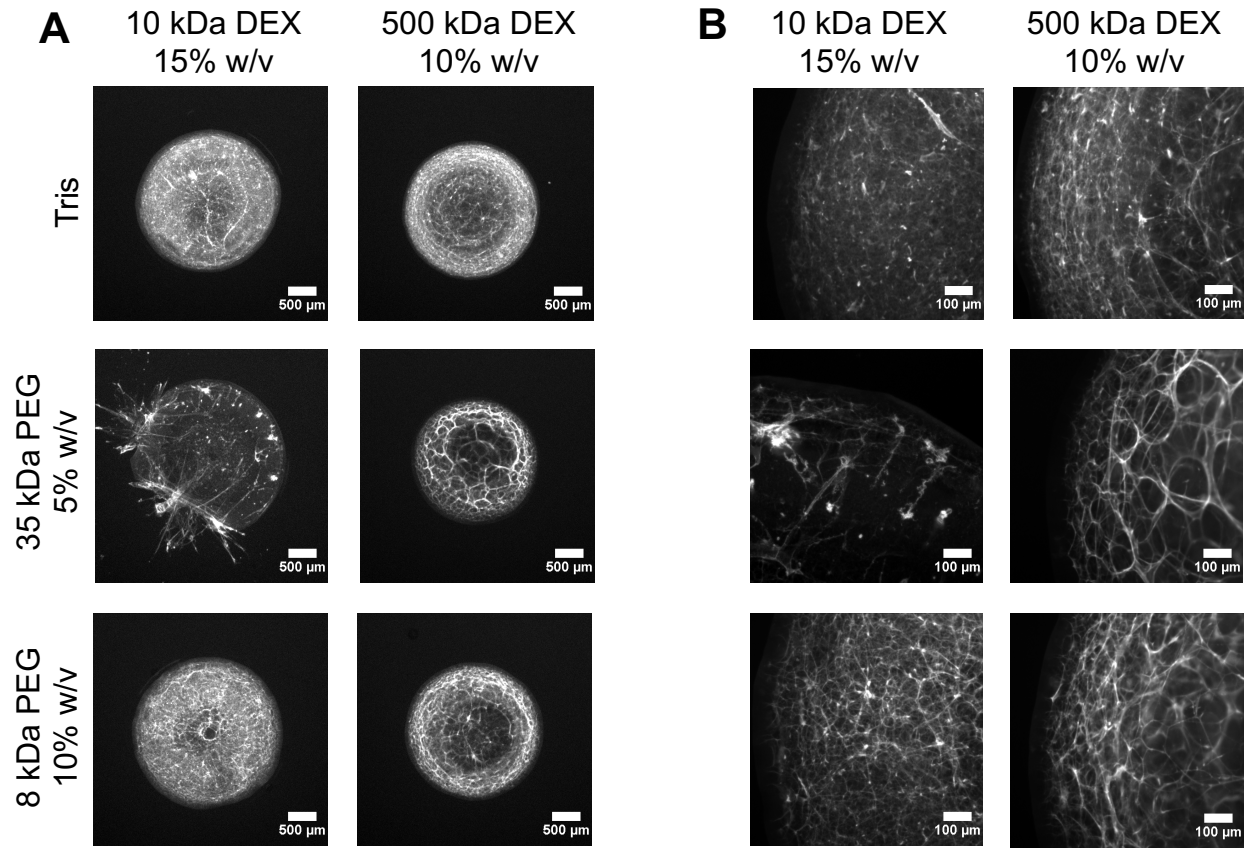
Figure 2-2: Determination of optimal ATPS parameters for DNA-histone structure formation

Two component molecular weights and concentrations of the ATPS-forming polymers DEX and PEG were combined with DNA and histones, respectively. After spotting a DEX-DNA droplet in a well and dehydrating, a solution of PEG-histone was washed over the well to rehydrate the DEX-DNA droplet and form a fibrous DNA-histone structure at the interface. Sytox Green was included in this PEG-histone solution such that the resultant structures could be visualized under a fluorescent microscope. (A) Structures visualized at low magnification (2x); (B) Structures visualized at high magnification (10x).
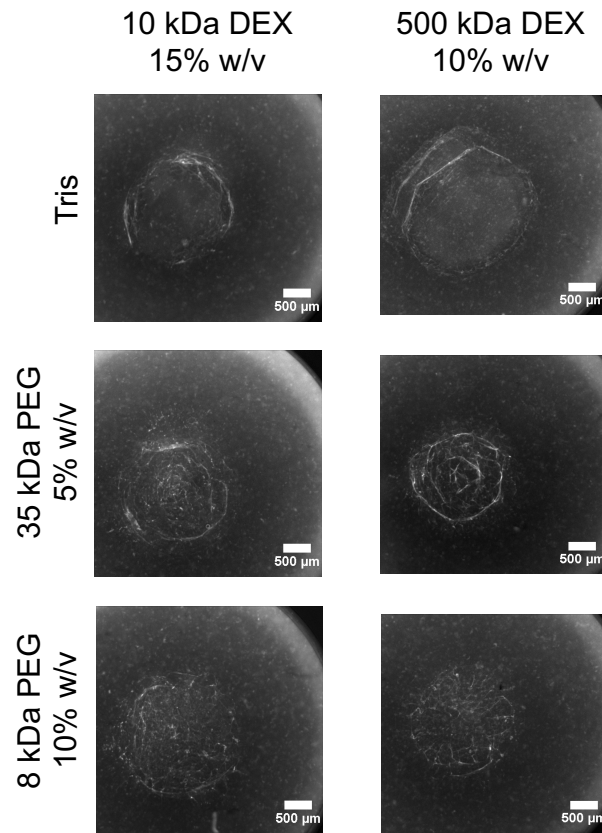
Figure 2-3: Inverted component-polymer assignments result in weak fibrous structures

Histone-DEX droplets were spotted on the surface of 96-well plates, dehydrated for 24 hours under vacuum, and rehydrated with DNA-PEG solution in a biological component-polymer assignment inversion from the previous iteration. Sytox Green was added to the DNA-PEG solution such that the resultant structures could be visualized under a fluorescent microscope.
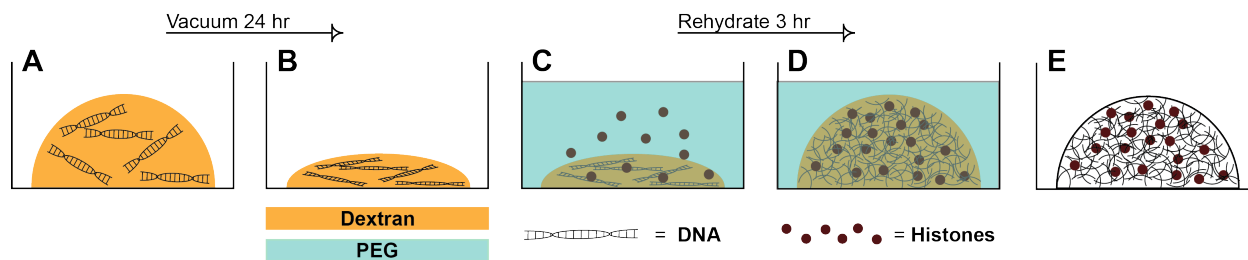
Figure 2-4: Final ATPS structure formation schematic

(A) DNA (methylated lambda phage, 100 ng/μL) in DEX (500 kDa, 10% w/v in 10 mM Tris-HCl) was spotted in 5 μL droplets in a 96-well plate. (B) The droplet was dehydrated by vacuum for 24 hours. (C) 100 μL of histones (calf thymus, 2 mg/mL) in PEG (35 kDa, 5% w/v in 10 mM Tris-HCl) was added to the well. (D) This solution was allowed to rehydrate for 3 hours. (E) The resulting structure was washed with multiple changes of 10 mM Tris-HCl, leaving 50 μL residual volume at all times.
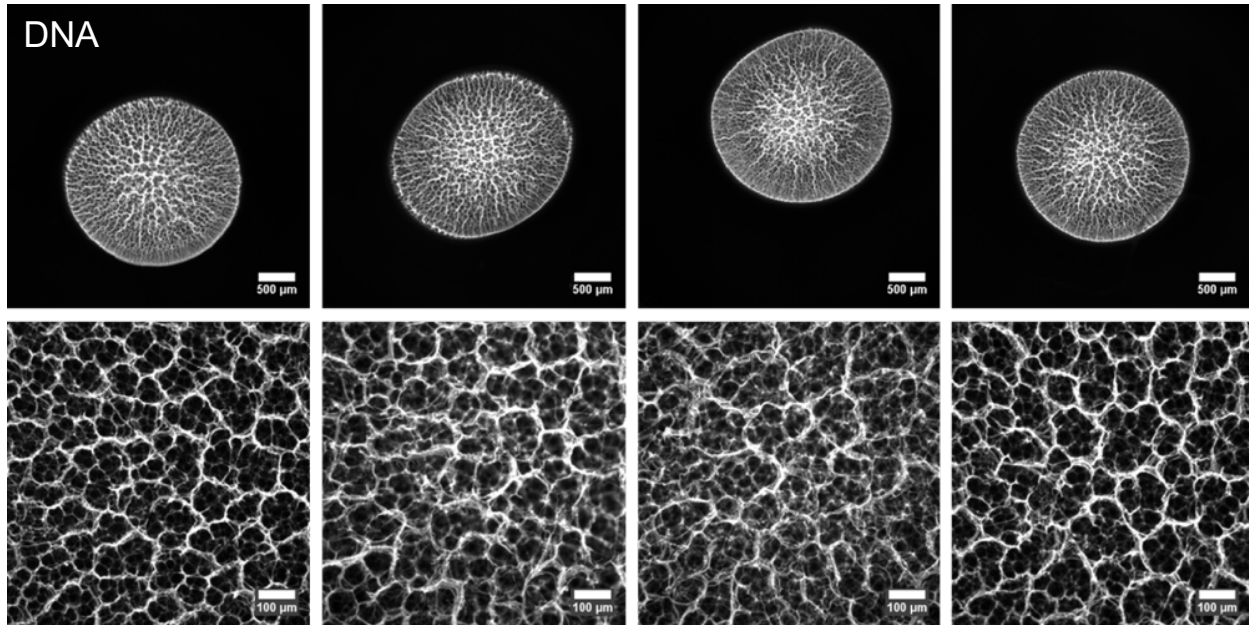
Figure 2-5: Optimized DNA-histone structure formation is reproducible

DNA-histone structures were generated by the aforementioned protocol in multiple wells of a 96-well plate and visualized by fluorescent microscopy. Presented here are four representative wells showing consistency both at low magnification (top row) and high magnification (bottom row).
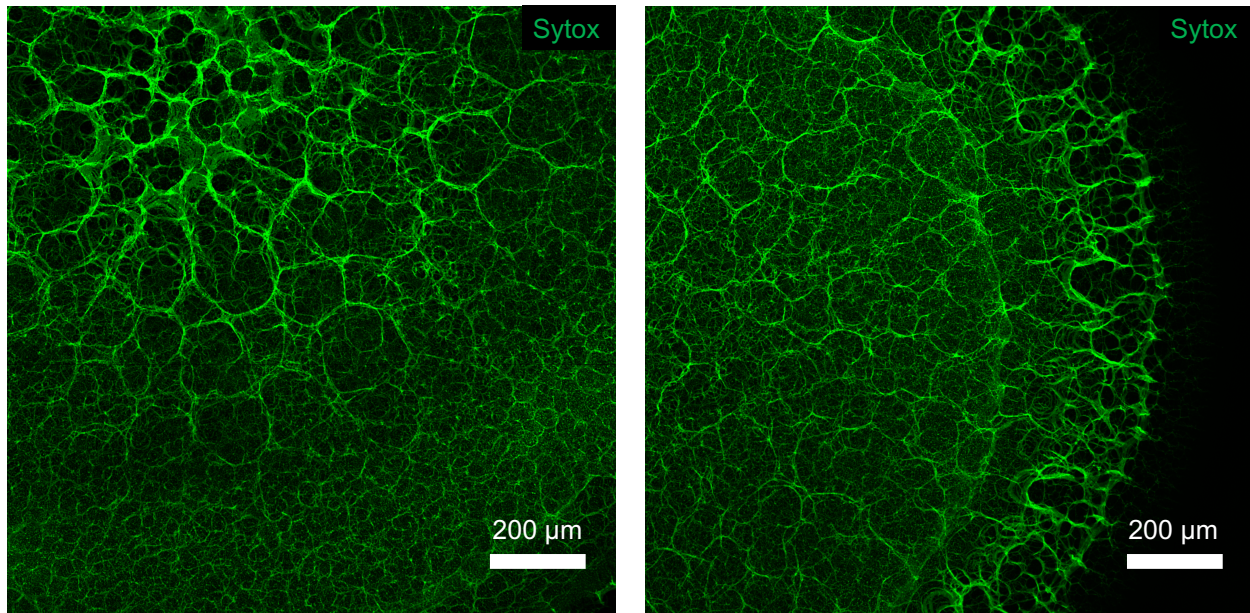
Figure 2-6: High-resolution microscopy reveals "nanofibrous" morphology of DNA-histone structures

ATPS-formed DNA-histone structures were fabricated as previously described, stained with Sytox Green, and visualized on a confocal microscope. Shown above are the fibrous morphology at the center of the structure (left panel) and the edge of the structure (right panel).
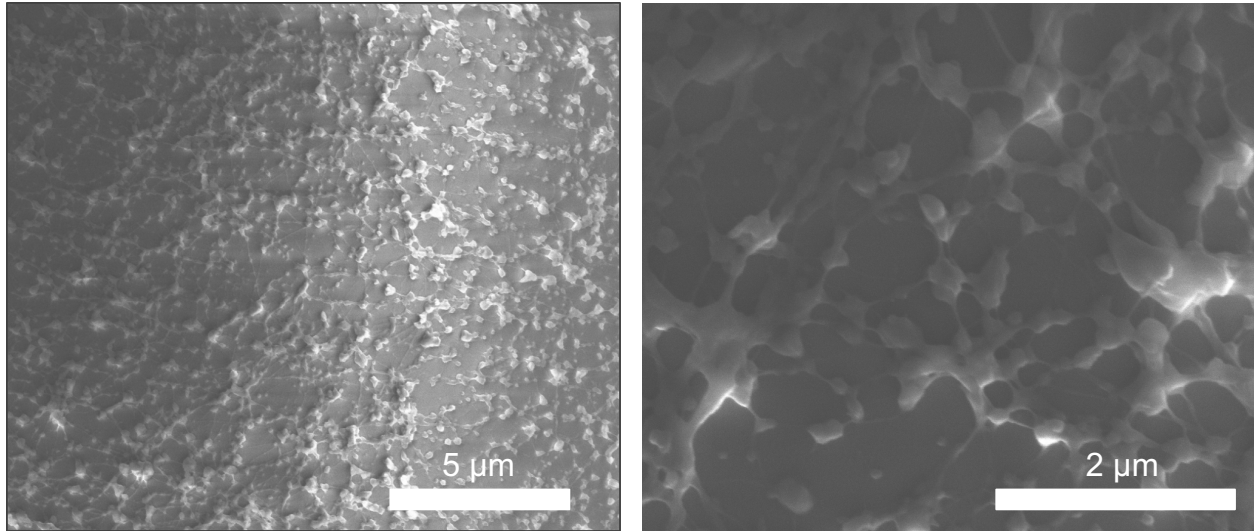
Figure 2-7: SEM reveals NET-like architecture of DNA-histone structures

ATPS-formed DNA-histone structures were fabricated as previously described, fixed, prepared via sequential ethanol dehydration and osmium tetroxide secondary fixation, and imaged via SEM.
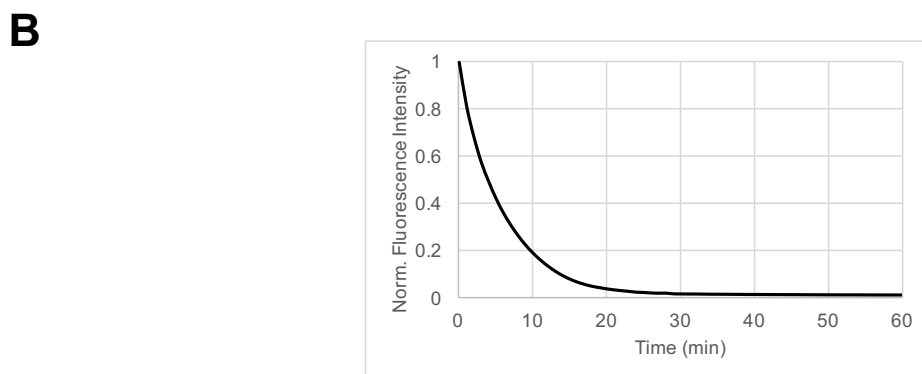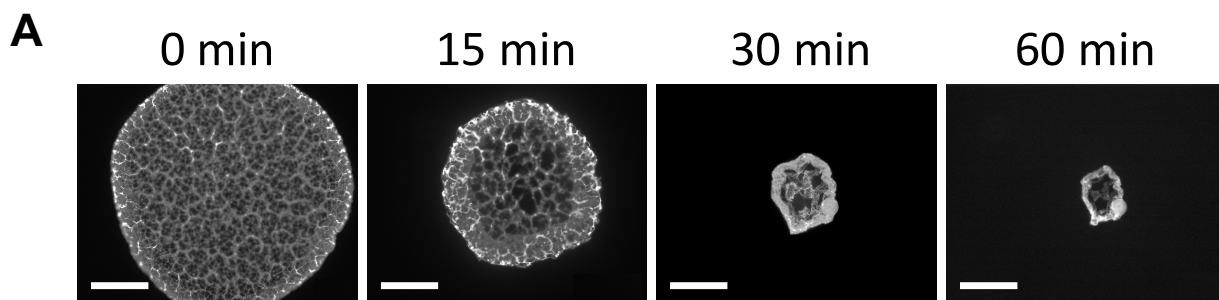
A

0 min   15 min   30 min   60 min

B

Figure 2-8: DNA-histone structure degradation can be monitored via microplate reader

DNA-histone structures were formed by ATPS as previously described, stained with Sytox Green, and subjected to degradation by 1 mg/mL DNase I at 37°C. The degradation process was monitored by (A) timepoint-based imaging, which was contrast-enhanced to show structural degradation at each time point, and (B) microplate reader measurements, normalized to the value at the initial time point. Scale bar represents 500 μm.
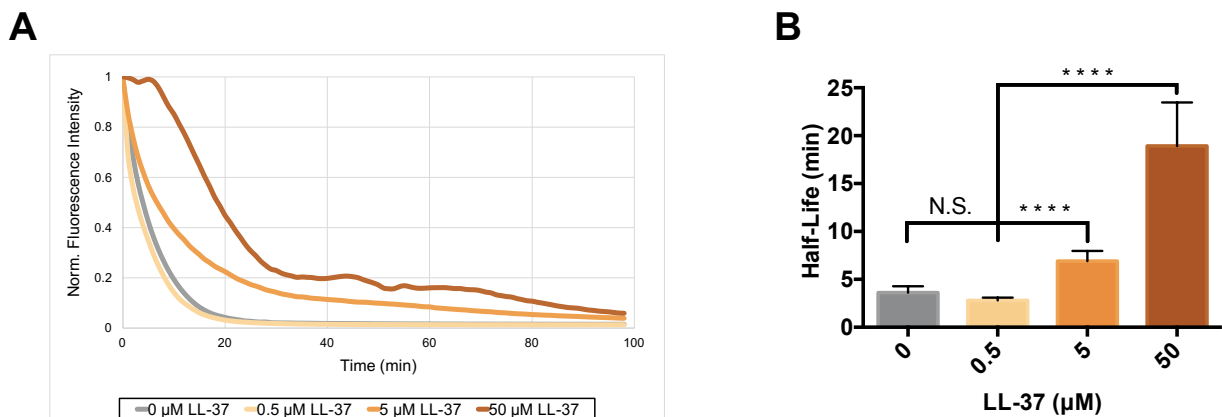
Figure 2-9: Addition of LL-37 increases DNA-histone structure degradation resistance in a dose-dependent manner

ATPS-formed DNA-histone structures were fabricated as previously described. After formation, LL-37 was applied at the indicated doses for one hour and washed away. Structures were then stained with Sytox Green and exposed to 1 mg/mL DNase I at 37°C. (A) Degradation was monitored via acquisition of microplate reader signal, normalized to the signal from the initial structure. Curves presented are means of $n = 3$ for each LL-37 containing condition and $n = 9$ for control. (B) Degradation behavior was quantified by the generation of the "Half-Life" metric, reporting time to a normalized fluorescence intensity I = 0.5. **** signifies $p < 0.0001$.

2.7　References

1.　Urban, C. F. *et al.* Neutrophil extracellular traps contain calprotectin, a cytosolic protein complex involved in host defense against Candida albicans. *PLoS Pathog.* **5**, e1000639 (2009).

2.　Lim, C. H. *et al.* Thrombin and Plasmin Alter the Proteome of Neutrophil Extracellular Traps. *Front. Immunol.* **9**, 1554 (2018).

3.　Khandpur, R. *et al.* NETs Are a Source of Citrullinated Autoantigens and Stimulate Inflammatory Responses in Rheumatoid Arthritis. *Sci. Transl. Med.* **5**, 178ra40-178ra40 (2013).

4.　Neumann, A. *et al.* Novel role of the antimicrobial peptide LL-37 in the protection of neutrophil extracellular traps against degradation by bacterial nucleases. *J. Innate Immun.* **6**, 860–868 (2014).

5.　Papayannopoulos, V., Metzler, K. D., Hakkim, A. & Zychlinsky, A. Neutrophil elastase and myeloperoxidase regulate the formation of neutrophil extracellular traps. *J. Cell Biol.* **191**, 677–691 (2010).

6.　Lewis, H. D. *et al.* Inhibition of PAD4 activity is sufficient to disrupt mouse and human NET formation. *Nat. Chem. Biol.* **11**, 189–191 (2015).

7.　Brinkmann, V., Laube, B., Abu Abed, U., Goosmann, C. & Zychlinsky, A. Neutrophil extracellular traps: how to generate and visualize them. *J. Vis. Exp. JoVE* (2010). doi:10.3791/1724

8.　Najmeh, S., Cools-Lartigue, J., Giannias, B., Spicer, J. & Ferri, L. E. Simplified Human Neutrophil Extracellular Traps (NETs) Isolation and Handling. *J. Vis. Exp. JoVE* (2015). doi:10.3791/52687

9.　Brinkmann, V. & Zychlinsky, A. Beneficial suicide: why neutrophils die to make NETs. *Nat. Rev. Microbiol.* **5**, 577–582 (2007).

10.　Netz, R. R. & Joanny, J.-F. Complexation between a Semiflexible Polyelectrolyte and an Oppositely Charged Sphere. *Macromolecules* **32**, 9026–9040 (1999).

11.　Kunze, K. K. & Netz, R. R. Salt-induced DNA-histone complexation. *Phys. Rev. Lett.* **85**, 4389–4392 (2000).

12.　Hatti-Kaul, R. Aqueous two-phase systems. A general overview. *Mol. Biotechnol.* **19**, 269–277 (2001).

13.　Tavana, H. *et al.* Nanolitre liquid patterning in aqueous environments for spatially defined reagent delivery to mammalian cells. *Nat. Mater.* **8**, 736–741 (2009).

14.　Frampton, J. P. *et al.* Rapid Self-Assembly of Macroscale Tissue Constructs at Biphasic Aqueous Interfaces. *Adv. Funct. Mater.* **25**, 1694–1699 (2015).

15.   Kwok, K. Y. *et al.* Strategies for maintaining the particle size of peptide DNA condensates following freeze-drying. *Int. J. Pharm.* **203**, 81–88 (2000).

16.   Pilsczek, F. H. *et al.* A novel mechanism of rapid nuclear neutrophil extracellular trap formation in response to Staphylococcus aureus. *J. Immunol. Baltim. Md 1950* **185**, 7413–7425 (2010).

17.   Brinkmann, V. Neutrophil Extracellular Traps Kill Bacteria. *Science* **303**, 1532–1535 (2004).

18.   Hakkim, A. *et al.* Impairment of neutrophil extracellular trap degradation is associated with lupus nephritis. *Proc. Natl. Acad. Sci. U. S. A.* **107**, 9813–9818 (2010).

19.   Leffler, J. *et al.* Neutrophil extracellular traps that are not degraded in systemic lupus erythematosus activate complement exacerbating the disease. *J. Immunol. Baltim. Md 1950* **188**, 3522–3531 (2012).